

Coherent Population Trapping Spectra in Presence of ac Magnetic Fields

G. Bevilacqua,¹ V. Biancalana,¹ E. Breschi,¹ Y. Dancheva,¹ L. Moi,¹ Ch. Andreeva,² S. Cartaleva,² and T. Karaulanov²

¹*Dipartimento di Fisica, Università di Siena, Via Roma 56, 53100 Siena, Italy*

²*Institute of Electronics, BAS, Boul. Tsarigradsko Shosse 72, 1784 Sofia, Bulgaria*

(Received 4 March 2005; published 14 September 2005)

Experimental and theoretical investigations are reported on the effects induced by an alternating magnetic field on coherent population trapping resonances. We show that the ac magnetic field produces sidebands of these resonances in such a way that the spectrum observed is similar to those observed via the FM spectroscopic technique. Because of the very narrow linewidth of the resonances, sidebands are resolved even for ac field frequencies as low as a fraction of a kHz. The theoretical model developed, which takes into account a very simple atomic structure, fits the experimental data quite well.

DOI: [10.1103/PhysRevLett.95.123601](https://doi.org/10.1103/PhysRevLett.95.123601)

PACS numbers: 42.50.Gy, 32.70.Jz, 42.50.Md

In this work we report on the results and theoretical interpretation of experiments on the coherent population trapping (CPT) effect produced in the presence of dc and ac magnetic fields. Coherent phenomena in atomic transitions are widely and intensively studied because of their attractive characteristic of producing extremely narrow spectral features in the optical domain [1]. CPT is observed when two coherent electromagnetic (e.m.) fields couple two ground states through an excited one (Λ system). CPT leads to a lack of fluorescence from the excited atoms or, conversely, vapor transparency [2,3]. Among various other applications, this effect is suitable for the realization of either atomic clocks [4,5] when the ground-state levels with magnetic quantum numbers $m_F = 0$ are involved, or very sensitive optical magnetometers if the ground levels have $m_F \neq 0$ [6,7].

So far, while the effect of a static magnetic field (MF) on CPT has been studied extensively [6,7], much less attention has been paid to the case of an alternating MF. Interesting results have recently been reported by Lukin *et al.* [8] and Yelin *et al.* [9]. In [8], the case of a coherent perturbation which couples the Λ system to a fourth state, giving rise to a doubling of the resonance, is discussed from a general point of view. In [9] the case of an alternating MF applied orthogonally to the laser beam is considered: such a field induces transitions between adjacent Zeeman ground sublevels which act as the fourth state needed to split the resonance.

In this work we consider a different configuration, where the ac MF is parallel to the laser beam propagation direction and to a bias static field. Very interesting modification of the CPT resonance line shapes is observed when the ac MF is switched on. The modified resonances resemble the spectra obtained when a single Λ system is probed with the frequency modulation (FM) technique in which the modulation frequency lies well outside the CPT linewidth. The FM spectroscopy [10–12] is a very sensitive technique where spectral structures are probed by a frequency modulated radiation. The spectrum of such radiation contains many components (sidebands) separated by the modulation

frequency Ω , which go separately in resonance. The detected radiation, due to discrimination by the structure of interest, contains unbalanced sidebands, producing signals at Ω (and harmonics) which can profitably be revealed by means of phase-sensitive amplifiers referenced to the modulating signal. The final output has a dispersion-shaped dependence on the frequency detuning.

In the present work similar features appear which can be explained in terms of “level sidebands” produced by the time-dependent term appearing in the Hamiltonian associated with the ac MF.

A sketch of the experimental setup is given in Fig. 1. The apparatus consists of a vertical cavity surface emitting laser (VCSEL) whose beam (circularly polarized) crosses a sealed Cs cell, buffered with Ne at 50 Torr. The cell is placed in a static homogeneous MF parallel to the laser beam. As an alkali specie, cesium has a level structure with a $^2S_{1/2}$ ground state split in two hyperfine levels having opposite Landé factors [13]. As a consequence, the MF removing the Zeeman degeneracy also causes a different displacement between the two arms of each Λ system depending on the magnetic quantum number m_F of the involved ground Zeeman sublevels. Thus the two arms of each Λ system go in resonance at frequencies differing by a constant term given by the hf separation (9.192 GHz in the case of Cs) plus a much smaller term proportional to $m_F|g_J|B$, where $|g_J|$ is the modulus of $^2S_{1/2}$ Landé factor and B is the amplitude of the applied MF. The VCSEL is frequency modulated at the half of the hyperfine ground-state level separation (≈ 4.6 GHz) and the modulating rf

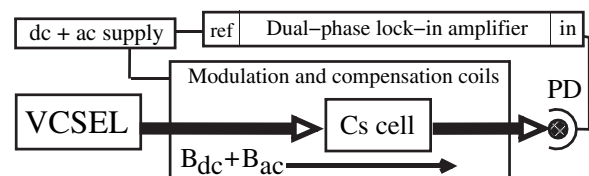


FIG. 1. Sketch of the experimental apparatus.

is swept in a small interval (a few tens of kHz) in order to detect the CPT resonances. In this way the first order sidebands produced in the laser spectrum are the two coherent optical e.m. fields needed for CPT. By keeping the modulation index small, the other sidebands can be neglected. The carrier frequency can also be neglected, because of its large detuning from the Cs hyperfine transitions. The buffer gas is added because it slows down the atom diffusion, increasing the laser-atom interaction time and allowing for observation of CPT resonances as narrow as a few hundred Hz. The stray dc MF components in the two directions perpendicular to the laser beam are canceled by two mutually orthogonal Helmholtz coils. A third Helmholtz pair is used to provide homogeneous longitudinal MF (B_{dc}) large enough to separate different Λ systems well. The cell is inside a solenoid that provides a longitudinal ac (B_{ac}) MF oscillating at Ω_{ac} . The CPT signal is monitored by collecting the transmitted light. Phase-sensitive detection is performed by means of a dual-phase lock-in amplifier referred to the ac current driving the alternating MF. Once the bias B_{dc} field amplitude is set, the CPT resonances are monitored by frequency sweeping the rf signal injected into the VCSEL. When a small B_{ac} field with a frequency in the hundred Hz range is applied and the rf modulation frequency is swept around 4.596 GHz, six narrow CPT resonances are observed. These resonances are due to Λ systems involving couples of ground-state Zeeman sublevels having $m_F \neq 0$ and are separated by an amount depending on B_{dc} . Here we report on the influence of the B_{ac} on a single one of those resonances, when the frequency and amplitude of the alternating field are increased. Our experimental results show that the six CPT resonances behave similarly in dependence on B_{ac} amplitude and frequency.

At low B_{ac} , by increasing Ω_{ac} , new spectral features appear in the CPT signal as shown in Fig. 2(a) where the line shapes clearly show two extra components displaced

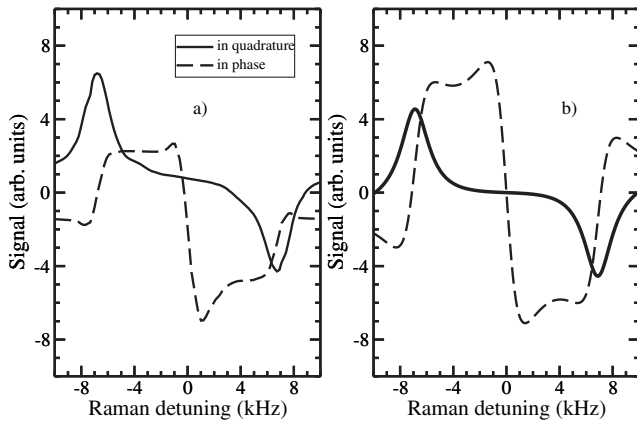


FIG. 2. The in-phase and in-quadrature signals as obtained experimentally (a) and calculated from the model (b): $B_{ac} = 1$ mG p - p and $\Omega_{ac} = 2\pi \times 6890$ Hz.

by an amount equal to $\pm\Omega_{ac}/2\pi$. Failache *et al.* [14] have recently reported similar behavior in a Hanle configuration experiment (degenerate two-level system), for small B_{ac} parallel to the laser beam. Extending our experimental investigations to the case of larger B_{ac} values, our (non-degenerate three-level) system shows that enhancing B_{ac} above a few mG results in observation of additional components in the CPT resonance spectrum, as we will show in the following.

For a theoretical analysis of the phenomenon observed, we propose a model based on a simplified three-level structure. In our conditions, due to the presence of dc MF, we have a set of Λ systems of form $|1\rangle = |F_e = 3, m_F - 1\rangle$, $|2\rangle = |F_g = 4, m_F\rangle$, and $|3\rangle = |F_g = 3, m_F\rangle$ giving resonances at different Raman detunings, corresponding to the different m_F values [15].

The various parameters used in the model and their meaning are shown in Fig. 3.

The dissipative part of the Liouvillian is taken into account in the following standard form

$$\mathcal{L}_{ij,km}^D = -\delta_{ik}\delta_{jm}\Gamma_{ij}(1 - \delta_{ij}) + \delta_{ij}\delta_{km}\left(\Gamma_{k\rightarrow i} - \sum_n \Gamma_{i\rightarrow n}\delta_{ki}\right), \quad (1)$$

where $\Gamma_{i\rightarrow j}$ are the population transition rates and the $\Gamma_{ij} = \Gamma_{ji}$ are the coherence damping parameters. A full list of the relaxation parameters used is shown in Table I. For a detailed discussion of these parameters and their numerical values, see, for instance, [16,17].

The Hermitian evolution is specified as follows (putting $\hbar = 1$)

$$H = \begin{pmatrix} E_1 + \omega_{1,B} & \Omega_1 & \Omega_2 \\ \Omega_1 & E_g + \omega_1 + \omega_{2,B} & 0 \\ \Omega_2 & 0 & -E_g + \omega_2 + \omega_{3,B} \end{pmatrix}, \quad (2)$$

where $\omega_{i,B} = m_i g_i \mu_B B_{ac} \cos\Omega_{ac}t$ is the Larmor frequency of the ac MF, Ω_i and ω_i are the Rabi and optical frequen-

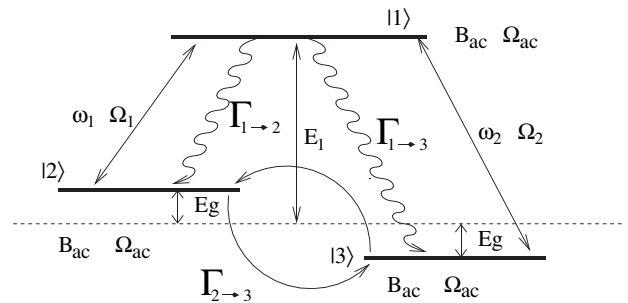


FIG. 3. Description of the model parameters used in the calculations. The states are $|1\rangle = |F_e, m_F - 1\rangle$, $|2\rangle = |F_g = 4, m_F\rangle$, and $|3\rangle = |F_g = 3, m_F\rangle$. The laser polarization is σ^- . The other relevant parameters are summarized in Table I.

TABLE I. The relaxation parameters used in the model. For a more detailed discussion see Refs. [16,17].

$\Gamma_{1\rightarrow 2}$	Spontaneous decay
$\Gamma_{1\rightarrow 3}$	Spontaneous decay
$\Gamma_{2\rightarrow 3} = \Gamma_{3\rightarrow 2}, \Gamma_{23}$	Diffusion through and collisions with the buffer gas, spin-exchange
Γ_{1i}	$\frac{1}{2}\Gamma_{1\rightarrow i} + \Gamma_{\text{buffer gas contribution}}$

cies of the two sidebands produced by the GHz rf modulation of the laser emission, m_i is the magnetic quantum number of the ground levels, and g_i their Landé factors. The effect of any static MF is included in E_g ; the interaction between the light and the atoms is taken in the rotating wave approximation and a reference frame which removes the optical oscillations $e^{-i\omega_1 t}$ and $e^{-i\omega_2 t}$ is used.

Using the normalization condition $\rho_{33} = 1 - \rho_{22} - \rho_{11}$ and arranging the density matrix ρ as a vector, the optical Bloch equations can be written as

$$\dot{\rho} = \mathcal{L}_0 \rho + 2\mathcal{L}_1 \cos(\Omega_{ac} t) \rho + \mathbf{w}, \quad (3)$$

where $\mathbf{w} = (0 \ 0 \ -i\Omega_2 \ 0 \ \Gamma_{3\rightarrow 2} \ 0 \ i\Omega_2 \ 0)$ while \mathcal{L}_0 and \mathcal{L}_1 are 8×8 noncommuting matrices, whose explicit forms can be obtained applying standard methods [18]. To get the solutions of equations (3) first we use a Floquet-Fourier expansion $\rho = \sum_{-\infty}^{+\infty} \rho_n e^{-in\Omega_{ac} t}$ and a similar expression for \mathbf{w} , thus obtaining in a straightforward way

$$\dot{\rho}_n = (\mathcal{L}_0 + in\Omega_{ac})\rho_n + \mathcal{L}_1(\rho_{n-1} + \rho_{n+1}) + \mathbf{w}\delta_{n,0}. \quad (4)$$

The steady-state solution ($\dot{\rho}_n^{SS} = 0$) can be obtained from the solution of the linear system in Eq. (4), which, as it is well known [see Chap. 9 of [19]], can be expressed by means of an infinite matrix continued fraction. Here we are only interested in $\rho_0^{SS} = (\mathcal{A}_0 - \mathcal{L}_1 \mathcal{G}_1 \mathcal{L}_1 - \mathcal{L}_1 \mathcal{G}_{-1} \mathcal{L}_1)^{-1} \mathbf{w}$ and $\rho_{\pm 1} = -\mathcal{G}_{\pm 1} \mathcal{L}_1 \rho_0^{SS}$, where $\mathcal{A}_n = \mathcal{L}_0 + in\Omega_{ac} \mathbb{1}_{8 \times 8}$ ($\mathbb{1}_{8 \times 8}$ is the identity matrix) and

$$\begin{aligned} \mathcal{G}_{\pm 1} &= \frac{1}{\mathcal{A}_{\pm 1} - \mathcal{L}_1(1/\mathcal{A}_{\pm 2} - \dots)\mathcal{L}_1} \\ &= \frac{1}{\mathcal{A}_{\pm 1} - \mathcal{L}_1 \mathcal{G}_{\pm 2} \mathcal{L}_1}. \end{aligned} \quad (5)$$

These matrix continued fractions (actually a truncation) can be summed in a straightforward way from bottom to top. We used a large enough truncation (with about a thousand partial denominators) in order to be sure that we did not miss any physical features.

The quantities of interest in order to make a direct comparison with the experimentally measured data are the absorption spectra. It is well known [20] that the absorption spectrum at ω_1 is $-\Im(\rho_{12})\Omega_1\omega_1$, while for the ω_2 component the relevant quantity is $-\Im(\rho_{13})\Omega_2\omega_2$. After a little algebra, we find

$$\begin{aligned} \Im(\rho_{12}) &= \Im(\rho_{12}^{(0)}) + \sum_{n=1}^{\infty} [\Im(\rho_{12}^{(n)} + \rho_{12}^{(-n)}) \cos(n\Omega_{ac} t) \\ &\quad - \Re(\rho_{12}^{(n)} - \rho_{12}^{(-n)}) \sin(n\Omega_{ac} t)]. \end{aligned} \quad (6)$$

It is easy to see that for the absorption at ω_1 the experimental in-phase and in-quadrature signals produced by a lock-in amplifier referenced to a signal at Ω_{ac} are proportional, respectively, to $A_{12} = \Im(\rho_{12}^{(1)} + \rho_{12}^{(-1)})$ and $B_{12} = \Re(\rho_{12}^{(-1)} - \rho_{12}^{(1)})$. Similar expressions hold for the absorption at ω_2 , and the total absorption is

$$A_{\text{total}} = -(A_{12}\Omega_1\omega_1 + A_{13}\Omega_2\omega_2) \quad (7a)$$

$$B_{\text{total}} = -(B_{12}\Omega_1\omega_1 + B_{13}\Omega_2\omega_2). \quad (7b)$$

Although the solution given by (5) is exact and very convenient for numerical calculations, a better insight into the physics of the system is achieved by transforming the initial Hamiltonian. In fact, defining the following time-dependent unitary transformation

$$U^\dagger = \begin{pmatrix} e^{-iS_1 \sin(\Omega_{ac} t)} & 0 & 0 \\ 0 & e^{-iS_2 \sin(\Omega_{ac} t)} & 0 \\ 0 & 0 & e^{-iS_3 \sin(\Omega_{ac} t)} \end{pmatrix} \quad (8)$$

and choosing

$$S_i = -m_i g_i \mu_B B_{ac} / \Omega_{ac}, \quad (9)$$

we get the following expression for the transformed Hamiltonian $H_t = U^\dagger H U + iU^\dagger \dot{U}$

$$H_t = \begin{pmatrix} E_1 & \Omega_1 e^{iM_2 \sin \Omega_{ac} t} & \Omega_2 e^{iM_3 \sin \Omega_{ac} t} \\ \Omega_1 e^{-iM_2 \sin \Omega_{ac} t} & E_g + \omega_1 & 0 \\ \Omega_2 e^{-iM_3 \sin \Omega_{ac} t} & 0 & -E_g + \omega_2 \end{pmatrix} \quad (10)$$

which is the Hamiltonian of a three-level system under the irradiation of two optical frequencies, each of which is frequency modulated with modulation index equal to

$$M_i = S_i - S_1 = (m_1 g_1 - m_i g_i) \frac{\mu_B B_{ac}}{\Omega_{ac}} \quad (11)$$

and modulation frequency Ω_{ac} . The Hamiltonian (10) exactly resembles that of the three levels irradiated with two polychromatic fields with frequencies $\omega_{1,n} = \omega_1 + n\Omega_{ac}$, $\omega_{2,m} = \omega_2 + m\Omega_{ac}$ and Rabi frequencies $\Omega_1 J_n(M_2)$,

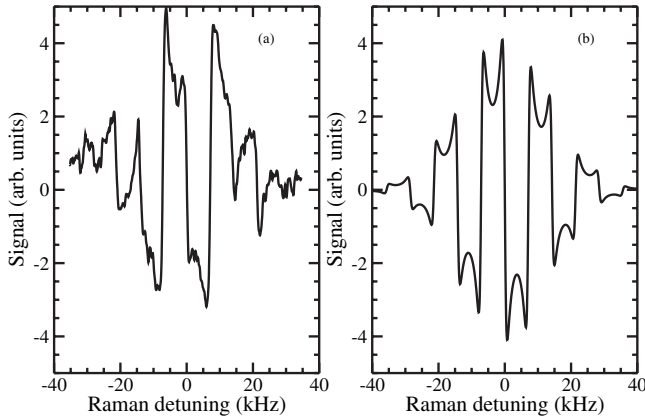


FIG. 4. The in-phase signal as obtained experimentally and from the simulation. The Zeeman degeneracy is removed by means of $B_{dc} = 138.4$ mG. The alternating field is $B_{ac} = 10.9$ mG and $\Omega_{ac} = 2\pi \times 7117$ Hz. The recorded signal comes from the Λ system involving $m_{F_g} = 2$ $m_{F_e} = 1$.

$\Omega_2 J_m(M_3)$, respectively, where $J_m(M_i)$ are the first-kind Bessel functions. In this sense (10) presents evident analogies with the Hamiltonian describing atomic samples in FM spectroscopy experiments. The main difference between the two cases consists in the fact that, according to (11), in our case the modulation indexes attributed to the two optical fields are, in general, different, and moreover they may have even opposite sign. As a consequence, it could be possible to combine our “level modulation” technique with a FM spectroscopy setup in order to separately and independently adjust the modulation indexes attributed to the optical field-hyperfine transition couple. From this point of view the proposed technique, used in conjunction with frequency modulated (at Ω_{ac}) radiation, can be used to enrich the set of accessible configurations of the effective spectral components in FM spectroscopy experiments. Even wider scenarios would be opened by using radiation modulated at a different frequency with respect to Ω_{ac} , where a sort of heterodyne signal could be created. Coming back to our case, where only the MF is alternating, the condition of zero Raman detuning for the (n, m) pairs of fields can be written as

$$\Delta_{n,m} = \omega_{1,n} - \omega_{2,m} - 2E_g = \Delta_{0,0} + (n - m)\Omega_{ac} = 0$$

and thus we expect to see a number of CPT lines separated by Ω_{ac} from both sides of the main line obtained with the pair of carriers $(0, 0)$. Notice that in this way we have also shown that, inversely, a frequency modulation of the lasers can be described to some extent as an effective ac MF on the levels.

In spite of the simplified level system considered in the model, a good correspondence is evident for most of the spectral features, and, in particular, the same number of side peaks is observed. In general, both in the experiment and in the model every new pair of side peaks appears at approximately the same M_i ratio. The frequency positions

of the experimental components coincide with the theoretical ones. Even for B_{ac} values larger than those presented in this Letter, the theory and the experiment are in qualitative agreement. In Fig. 4, for instance, the in-phase signal is plotted versus the Raman detuning for a particular value of B_{ac} . Of course, a quantitative analysis would demand the use a more complex model, including the whole set of levels. We actually plan to extend the work in this direction, also with the aim of accounting for minor but interesting observations, such as the sign reversal that appears for some components, which can be seen for the third order peaks in the case of Fig. 4.

The authors are pleased to acknowledge the financial support of the European Union (Contract No. G6RD-CT-2001-00642). The authors wish to thank E. Thorley for her kind collaboration in improving the manuscript.

- [1] E. Arimondo, *Prog. Opt.* **35**, 257 (1996).
- [2] G. Alzetta, A. Gozzini, L. Moi, and G. Orriols, *Nuovo Cimento Soc. Ital. Fis. B* **36**, 5 (1976).
- [3] S. E. Harris, *Phys. Today* **50**, No. 7, 36 (1997).
- [4] L. Hollberg, S. Knappe, and R. Wynands, *Electron. Lett.* **37**, 1449 (2001).
- [5] S. Knappe, L. Hollberg, and J. Kitching, *Opt. Lett.* **29**, 388 (2004).
- [6] R. Wynands and A. Nagel, *Appl. Phys. B* **68**, 1 (1999).
- [7] C. Affolderbach, M. Staehler, S. Knappe, and R. Wynands, *Appl. Phys. B* **75**, 605 (2002).
- [8] M. D. Lukin, S. F. Yelin, M. Fleischhauer, and M. O. Scully, *Phys. Rev. A* **60**, 3225 (1999).
- [9] S. F. Yelin, V. A. Sautenkov, M. M. Kash, G. R. Welch, and M. D. Lukin, *Phys. Rev. A* **68**, 063801 (2003).
- [10] W. Demtröder, *Laser Spectroscopy* (Springer-Verlag, Berlin, 2002), 3rd ed..
- [11] J. L. Hall, L. Hollberg, T. Baer, and H. G. Robinson, *Appl. Phys. Lett.* **39**, 680 (1981).
- [12] G. C. Bjorklund, M. D. Levenson, W. Lenth, and C. Ortiz, *Appl. Phys. B* **32**, 145 (1983).
- [13] D. A. Steck, <http://steck.us/alkalidata/>.
- [14] H. Failache, P. Valente, G. Ban, V. Lorent, and A. Lezama, *Phys. Rev. A* **67**, 043810 (2003).
- [15] Similar results are also obtained when the model is applied the case of excited state $|e\rangle = |F_e = 4, m_F \pm 1\rangle$, which has a different Landé factor.
- [16] J. Vanier and C. Audoin, *The Quantum Physics of Atomic Frequency Standards* (Adam-Hilger, Bristol, England, 1989).
- [17] A. Godone, F. Levi, and S. Micalizio, *Coherent Population Trapping Maser* (Edizioni C.L.U.T., Torino, 2002).
- [18] The equations for the eight independent density matrix elements can be recast in the form (3) by a relabeling procedure, for instance $\rho_{11} \rightarrow \rho_1, \rho_{12} \rightarrow \rho_2, \dots, \rho_{32} \rightarrow \rho_8$.
- [19] H. Risken, *The Fokker-Planck Equation*, Springer Ser. Synergetics (Springer-Verlag, Berlin, 1989), 2nd ed..
- [20] C. Choen-Tannoudji, J. Dupont-Roc, and G. Grynberg, *Atom-Photon Interactions: Basic Processes and Applications* (Wiley-Interscience, New York, 1998).